

Proactive Optimal Variable Speed Limit Control for Recurrently Congested Freeway Bottlenecks

By

Xianfeng Yang (Corresponding Author)

Ph.D Candidate

Department of Civil & Environmental Engineering
University of Maryland
1173 Glenn L. Martin Hall, College Park, MD 20742
Tel: (301)-405-2638
Email: xyang125@umd.edu

Yang (Carl) Lu

Ph.D Candidate

Department of Civil & Environmental Engineering
University of Maryland
1173 Glenn L. Martin Hall, College Park, MD 20742
Tel: (301)-405-2638
Email: yanglu@umd.edu

Gang-Len Chang

Ph.D., Professor

Department of Civil & Environmental Engineering
University of Maryland
1173 Glenn L. Martin Hall, College Park, MD 20742
Tel: (301)-405-2638
Email: gang@umd.edu

Word Count: $5000 + (9 \text{ Figures} + 1 \text{ table}) * 250 = 7,500$ words

2013 Transportation Research Board 92nd Annual Meeting

Paper #: 13-3139

1 **ABSTRACT**

2 This study presents two models for proactive VSL control on recurrently congested freeway segments.
3 The proposed basic model uses embedded traffic flow relations to predict the evolution of congestion
4 pattern over the projected time horizon, and computes the optimal speed limit. To contend with the
5 difficulty in capturing driver responses to VSL control, this study also proposes an advanced model
6 that further adopts Kalman Filter to enhance the accuracy of traffic state prediction. Both models have
7 been investigated with different traffic conditions and different control objectives. Our extensive
8 simulation analysis with a VISSIM simulator, calibrated with field data from our previous VSL
9 demonstration site, has revealed the benefits of the proposed VSL control model, compared with the
10 case without VSL. Also the results indicated that both proposed proactive models can outperform the
11 basic models and significantly reduce the travel time as well as number of stops over the recurrent
12 bottleneck locations. With respect to several selected MOEs, such as average number of stops and
13 average travel time, it has been found that the one with the control objective of minimizing speed
14 variance clearly outperforms other models.

1 INTRODUCTION

2 VSL is initially designed to reduce the speed difference on some hazardous highway segments, so as
3 to decrease the rear-end collision rate and improve traffic safety (1-3). Recently, it has been
4 recognized that VSL may offer the potential to mitigate traffic congestion and improve traffic
5 efficiency at work-zones and freeway bottlenecks. Through properly displayed and dynamically
6 changed speed limit along a controlled segment, VSL can smooth the transition between the upstream
7 and congested downstream flows to minimize the impact of shockwave on traffic conditions. The
8 mitigation of stop-and-go traffic speed variance can facilitate traffic flows to better utilize the
9 available roadway capacity during peak periods.

10 Despite the potential benefits of VSL for recurrent congestion, design of reliable algorithms
11 to ensure its benefits remains a challenging issue. For example, the Dutch VSL experiment (5)
12 showed no improvement in capacity which may be attributed to its advisory purpose. Bertini (6)
13 analyzed the data obtained from German Autobahn 9 (A9) near Munich, Germany and found strong
14 correlations between the VSL and traffic condition dynamics at bottleneck locations. More recently,
15 Chang et al. (7) reported a successful implementation of an integrated VSL and travel time
16 information system on MD 100 near Coca-Cola Drive which achieved travel time and throughput
17 improvements.

18 Along the same line, a study on the I-495 Capital Beltway (8) revealed that VSL can delay
19 the formation of bottleneck congestion. Abdel-Aty et al. (9, 10) developed a VSL system for I-4
20 through Orlando, Florida and reported to reduce both crash risk and travel time under a simulated
21 environment. Hegyi et al. (11, 12) modified the METANET macroscopic traffic flow model to
22 incorporate the VSL effect and adopted the model predictive control (MPC) approach to determine
23 the optimal speed limit. Papageorgiou et al. (13) and Carlson et al. (14) analyzed the effect of VSL on
24 aggregated traffic flow behavior from the theoretical perspective, and proposed an open-loop
25 integrated optimal control framework to coordinate ramp metering with VSL control. Their
26 simulation results show a reduction of 15 percent in total travel time. Most recently, Hadiuzzaman et
27 al. (15) proposed a modified CTM based VSL control and also used the model predictive control
28 (MPC) method to dynamically change the speed limit in real time. Their VISSIM simulation results
29 showed a reduction of 15-17 percent in travel time and flow rate.

30 In brief, most reactive control algorithms reported in the literature show some difficulty in
31 improving the traffic flow efficiency, while most proactive models seem to yield better control results.
32 Hence, further exploration of the proactive VSL control will be essential for its effective
33 implementation on recurrently congested highway segments. Some priority research issues to be
34 addressed include the effect of prediction accuracy of traffic conditions on a VSL's effectiveness, and
35 the best control objective to maximize the operational efficiency. This study proposed two types of
36 VSL model in response to these issues: a basic model based on the modified macroscopic traffic flow
37 model (16, 17), and an advanced model with its prediction function enhanced by Kalman Filter. Each
38 VSL model has been tested with two control objectives: total travel time minimization and speed
39 variance minimization.

40 This paper is organized as follows: The key features of the proposed VSL system are briefly
41 described in the next section. Formulations of the basic proactive are introduced in Section 3. Section
42 4 addresses the design of the traffic state estimator, based on the Kalman filtering methodology,
43 followed by presentation of the enhanced VSL model. Design of simulation experiments for
44 evaluating the performance of our proposed models under simulated real-time control environments is
45 reported in Section 6. Conclusions and future research are summarized in the last section.

VSL SYSTEM DESCRIPTION

As shown in FIGURE 1, due to the perceived congestion the upstream approaching vehicles are often forced to slow down before reaching the bottleneck. The formation of bottleneck may be caused by various factors such as lanes reduction or weaving maneuvers from heavy off-ramp flows. Without proper control, the approaching vehicles are likely to slow their speeds abruptly just upstream of the bottleneck location, often dropping from a “free-flow” to “stop-and-go” conditions and consequently producing shockwaves to reduce the throughput as well as the speed over the bottleneck segment. The VSL proposed in this study is designed to mitigate such shockwave impacts and to best use the available roadway capacity of the congested segment.

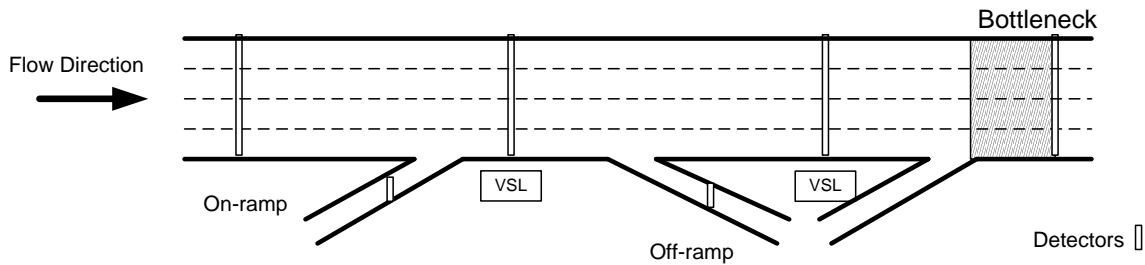


FIGURE 1 Configuration of a VSL system

The proposed VSL system consists of detectors, variable speed limit signs, and a central processing unit to execute control actions. For a target freeway stretch, the upstream detector is used to capture the free-flow arrival rate, and a downstream detector is designed to record the discharging rate from the bottleneck. Also, additional detectors are placed at those on-ramps and off-ramps to record ramp arriving and departing flows. Several VSL signs along with detectors would be installed between the upstream and downstream detectors. In a field application, those VSL signs will dynamically update their displayed speed limit based on the computed optimal set of speeds and the specified criteria for VMS display.

Depending on the approaching volume, driver compliance rate, and the resulting congestion along the target freeway segment, a VSL system’s central processing unit is responsible to produce the time-varying optimal speed limits. Note that for the safety concern and effective communications with drivers, all displayed speed limits are supposed to remain unchanged over the length of T^c seconds.

BASIC PROACTIVE CONTROL MODEL

The operational structure of the proposed VSL control system includes the following two principal components:

- **Macroscopic Traffic Flow Model:** Given the detected upstream flow rate and downstream discharging rate, the traffic flow model is used to predict the traffic state evolution in each freeway subsection;
- **Optimization model:** Based on the predicted conditions from traffic flow model, the optimization model is adopted to find the optimal set of speed limits with respect to a specified objective function.

For convenience of discussion, the control variables and parameters are listed below:

- Control time and subsection index
 - ΔT : Unit time interval for control operations;
 - T^P : Time interval for prediction horizon;
 - T^C : Time interval for control horizon;
 - k : Time interval index for control operation;
- Network geometric and physical data
 - Δl : Length of each freeway segment;
 - n_i : Number of lanes in subsection i ;
- Traffic states
 - $q_i(k)$: Transition flow rate entering segment (i-1) from segment i during interval k ;
 - $r_i(k)$: On-ramp flow rate entering segment i during interval k ;
 - $s_i(k)$: Off-ramp flow rate entering segment i during interval k ;
 - $Q_i(k)$: Average flow rate in segment i during interval k ;
 - $d_i(k)$: Mean traffic density in segment i during interval k ;
 - $u_i(k)$: Mean speed in segment i during interval k ;
- Control variables and boudaries
 - $v_i(k)$: Variable speed limit ratio in segment i during interval k ;
 - d_j : Jam traffic density;
 - u_f : Minimum mean speed;
 - d_c : Critical traffic density;
 - $u_f(k)$: Free flow speed;
- Model Parameters
 - α_i : Transition flow weigh factor;
 - β_i, γ : Speed-density adjustment factor;
 - v, τ, κ : Traffic state model parameter.

Macroscopic Traffic Flow Model

To perform a proactive dynamic VSL control, a reliable prediction model is essential to predict the traffic state evolution under the detected traffic conditions and driver responses. This study employs a calibrated traffic flow model to predict traffic conditions over the target time horizon and to provide the essential information for the VSL optimization module.

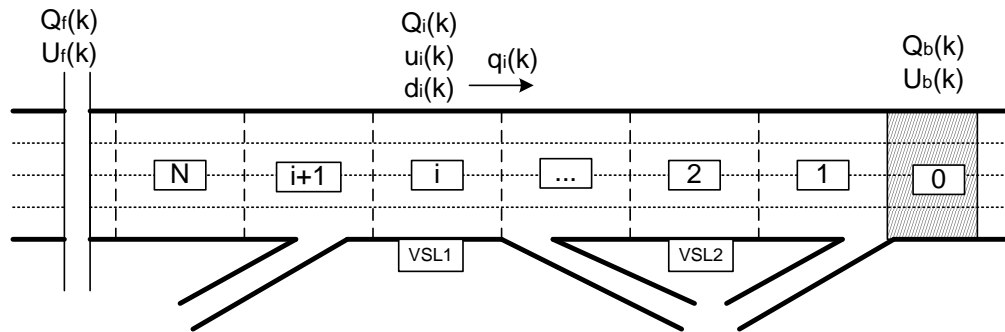


FIGURE 2 Typical freeway segments

As shown in FIGURE 2, for convenience of computation, the target freeway segment is divided into N subsections with a unit length of Δl . While dividing a freeway segment into subsections, the length of subsections should be sufficiently long so that vehicles cannot pass one subsection during one time interval k . Moreover, each subsection is allowed to have at most one on-ramp and one off-ramp. For each subsection i , the mean density, $d_i(k)$, can be determined by the difference between the input and output flows as follows:

$$d_i(k) = d_i(k-1) + \frac{\Delta T}{\Delta l * n_i} [q_{i+1}(k) - q_i(k) + r_i(k) - s_i(k)] \quad (1)$$

The transition flow rate is determined by the mean speed, density, the capacity of target segment, and the remaining capacity of the downstream segment, that is:

$$q_i(k) = \text{Min}\{\alpha_i Q_i(k) + (1 - \alpha_i) Q_{i-1}(k), q_{\max} n_i, (d_j - d_{i-1}(k)) n_i \gamma\} \quad (2)$$

where, α_i (transition flow weight factor) can be calibrated with field measurements. Wu and Chang (17) stated that it should lie in the interval [0.5,1.0].

For the average speed, $u_i(k)$, one can also establish its evolution relation with the following properly selected speed-density relation and shock-wave formation equations:

$$u_i(k) = u_i(k-1) + \beta_i \{S[d_i(k-1)] - u_i(k-1)\} + g_i(k-1) \quad (3)$$

The second component describes an adaptation of the average speed to the speed-density characteristics, as:

$$S[d_i(k), v_i(k)] = \begin{cases} u_i^f & \text{if } d_i(k) \leq d_c \\ u_i^f \cdot \frac{(\frac{d_j}{d_i(k)} - 1)}{(\frac{d_j}{d_c} - 1)} & \text{if } d_i(k) > d_c \end{cases} \quad (4)$$

Eq.(4) was originally formulated by Hadiuzzaman (15); and the third component $g_i(k)$ of Eq.(3) takes into account the density difference between downstream and upstream segments (18), that is:

$$g_i(k) = \frac{v \Delta T}{\tau \Delta l} \cdot \frac{d(i-1, k) - d(i, k)}{d(i, k) + \kappa} \quad (5)$$

Constraints

In a field application, drivers may begin to reduce the speed when they perceive the VSL sign. Therefore, assuming a driver's perception distance to be Δl , the target controlled area shall start from one segment ahead of the VSL location (e.g., as shown In FIGURE 2, the controlled area with VSL-2 includes segment 0 to segment 3; the controlled sections with VSL-1 are segment 4 to segment $i+1$).

For each subsection i , the mean speed shall be constrained by:

$$\begin{cases} u_J \leq u_i(k) \leq u_f, & \text{segment } i \text{ without VSL control;} \\ u_J \leq u_i(k) \leq u_f v_i(k), & \text{segment } i \text{ with VSL control.} \end{cases} \quad (6)$$

And,

$$0 < v_i(k) \leq 1 \quad (7)$$

In view of the jam density, one shall also set the density boundaries as follows:

$$0 \leq d_i(k) \leq d_J \quad (8)$$

Also, for safety concern the speed variation between consecutive intervals is set to be within the following boundaries.

$$-\delta \leq u_i^f v_i(k) - u_i^f v_i(k-1) \leq \delta \quad (9)$$

where, δ is the maximum allowable difference between two successive speed displays on VMS.

Objective Functions

As the primary focus of VSL is to increase traffic flow speed and its stability, this study first adopts the following minimization of total travel time over the controlled segment as the objective function:

$$\min \sum_k \sum_i n_i d_i(k) \Delta T \quad (10)$$

Note that depending on the response of drivers to the displayed speeds, the embedded macroscopic traffic flow models and the above objective function may not fully capture the complex traffic dynamics and yield the true optimal results.

Some existing studies report that a proper VSL control can help smooth speed transition, which will consequently reduce the number of vehicle stops and shockwave impact on the traffic conditions (7). Hence, this study has further explored the following objective function of minimizing the speed variance along the target freeway for a VSL control:

$$\min \sum_k \sum_i (u_i(k) - u_{ave})^2 \quad (11)$$

where, u_{ave} is the average speed of the target freeway stretch, and is given as follows:

$$u_{ave} = \frac{\sum_k \sum_i u_i(k)}{(T^c / \Delta T) \cdot N} \quad (12)$$

For safety concern the speed variation between consecutive intervals is limited within a given range, as Shown in Eq. (9). Therefore, the feasible solution set is quite small and one can thus adopt enumerative search for the optimal solution.

ENHANCED PROACTIVE CONTROL MODEL

To fully capture the complex interrelations between speed and density, this study has further adopted the Kalman Filter to improve the accuracy of the predicted traffic conditions over the target time horizon for proactive VSL control. The Kalman Filter is an optimal state estimator applied to a dynamic system that involves random noise and includes a limited amount of noisy real-time measurements. The correction and update process of a typical Kalman Filter process is summarized in FIGURE 3:

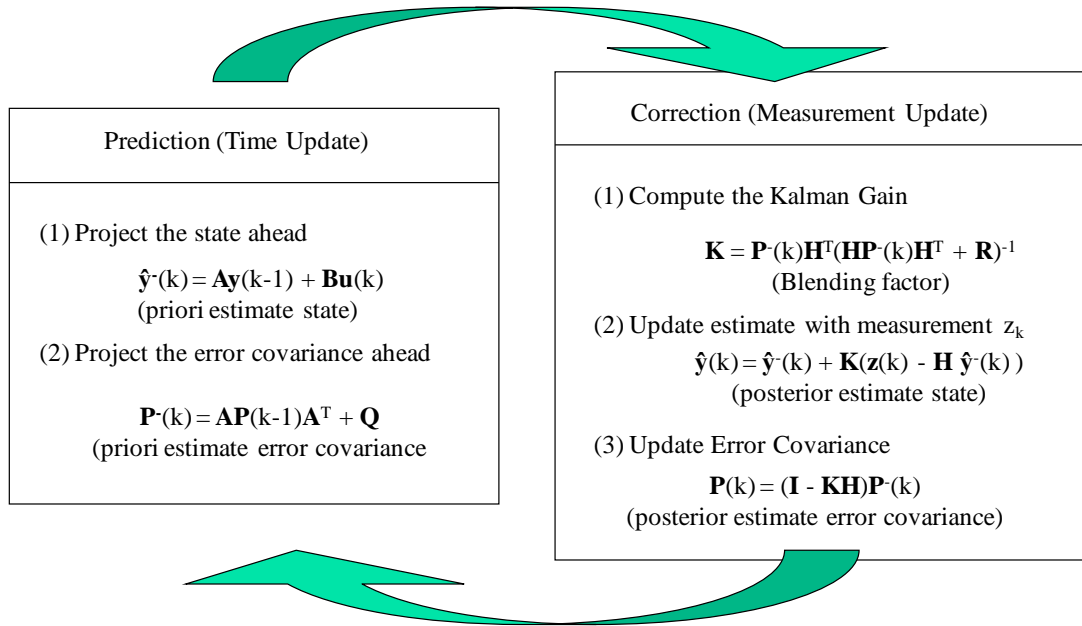


FIGURE 3 An Illustration of Kalman Filter Correction and Update Process

where, $\mathbf{y}(k)$ is the estimated traffic state vector, and $\mathbf{u}(k)$ is the system input:

$$\mathbf{y}(k) = [q_1(k) \ u_1(k) \ q_2(k) \ u_2(k) \ \cdots \ q_N(k) \ u_N(k)]^T$$

$$\mathbf{u}(k) = [q_0(k) \ v_0(k) \ q_{N+1}(k) \ v_{N+1}(k) \ r_1(k) \ \cdots \ r_N(k) \ s_1(k) \ \cdots \ s_N(k)]^T$$

$\mathbf{z}(k)$ is the vector of measurement, and has the following relation with $\mathbf{y}(k)$:

$$\mathbf{z}(k) = \mathbf{H}\mathbf{y}(k) + \mathbf{v}(k) \tag{14}$$

where, $\mathbf{v}(k)$ is the measurement error.

By using Kalman Filter, the predicted traffic state can be constantly updated based on the detector data, and the new optimal speed limits can then be generated with the proposed optimization model.

As mentioned in Section 2, to prevent confusing drivers, the displayed speed limits are not allowed to change frequently. Therefore, by defining a control horizon T^C , the speed limits will remain unchanged over the specified time interval. Also note that the optimization model will be activated once all detector data have been updated, where the control horizon is normally equal to the length of multiple detector update intervals. Therefore, during each control horizon, the optimization model will produce multiple estimates of the optimal speed limit, and the process to select the robust one prior to its execution is shown below.

For example, assuming that the VSL's display interval (control horizon) is set as 5 minutes and the detector data is updated at every 1 minute, then each control interval will have five sets of estimated optimal speed limits prior to its implementation time, as shown in FIGURE 4.

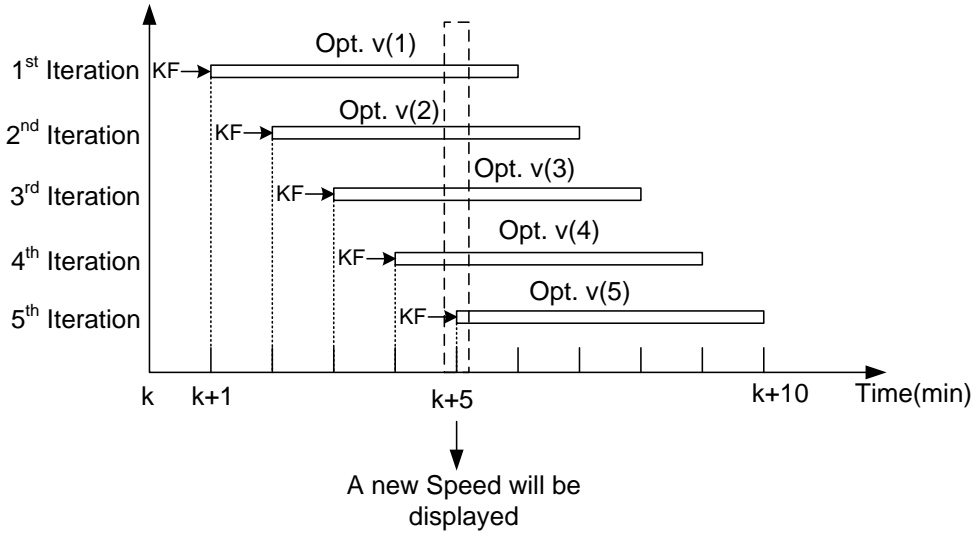


FIGURE 4 An example of the VSL control Strategy

Given the set of computed optimal speed limits for the same horizon, $\{v(1), v(2), \dots, v(n)\}$, one can determine the speed limits to be displayed based on the following procedure as used in most online systems (19):

- 1) Define a counter M to identify the moving direction of the speed limit, and then denote v^t as the displayed speed limit of the current horizon, where M is updated by the following expression:

$$M = \begin{cases} M + 1, & \text{if } v(i) > v^t \\ M, & \text{if } v(i) = v^t, \quad i=1, 2, \dots, n; \\ M - 1, & \text{if } v(i) < v^t \end{cases} \quad (15)$$

- 2) The new displayed speed limit for the next horizon will be readjusted with the predetermined increment Δ , based on the value of M :

$$v^{t+1} = \begin{cases} v^t + \Delta, & \text{if } M > 0 \\ v^t, & \text{if } M = 0 \\ v^t - \Delta, & \text{if } M < 0 \end{cases} \quad (16)$$

In summary, the entire proactive control process includes the following primary steps:

- Step 0: Divide the target freeway segment into a set of subsections and then deploy the VSL signs and detectors; determine the length of control time interval.
- Step 1: Apply the Kalman Filter module to revise the predicted traffic conditions produced from the macroscopic traffic model, and execute the optimization model to generate a new set of optimal speed limits for each detector data update interval.
- Step 2: Update the counter M by comparing the new optimal speed limit with the current displayed speed, (see Eq.(15)).
- Step 3: Select the new speed limits to display, based on Eq.(16).
- Step 4: Stop the VSL operations if traffic flow speed has evolved back to its normal prevailing speed.

The operational flow chart of the VSL control system is presented in FIGURE 5:

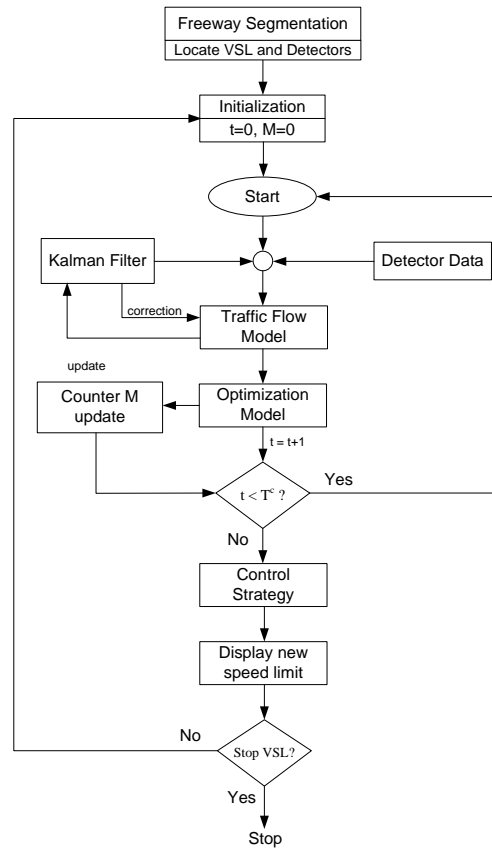


FIGURE 5 Flow chart of the enhanced proactive model VSL control system

SYSTEM EVALUATION

Case Description

To evaluate the proposed optimization models, this study selected the segment MD-100 West from MD 713 to Coca-Cola Drive, our previous VSL field demonstration site, for simulation analysis. On typical weekdays, the speed during the peak hours usually drops quickly from 60 to 20 mph (e.g., in 5 mins) after the onset of congestion, and recovers to about 40 mph after passing Coca-Cola Drive.

Using the field data collected on Dec. 19, 2009, FIGURE 6(A) illustrates the spatial evolution of traffic flow speeds on the target MD-100 segment and FIGURE 6(B) shows the travel time evolution at the target segment over the AM peak hours.

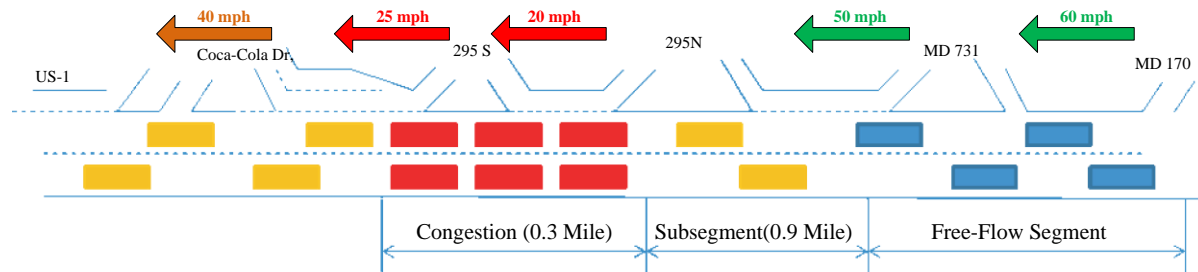


FIGURE 6(A) Spatial evolution of traffic flow speeds on the target MD-100 segment

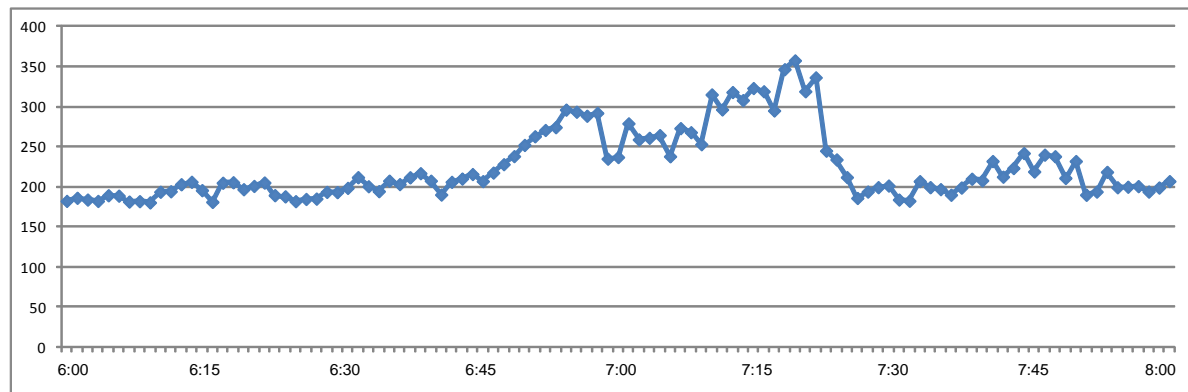


FIGURE 6(B) Travel time evolution of the target MD-100 segment during AM Peak Hours

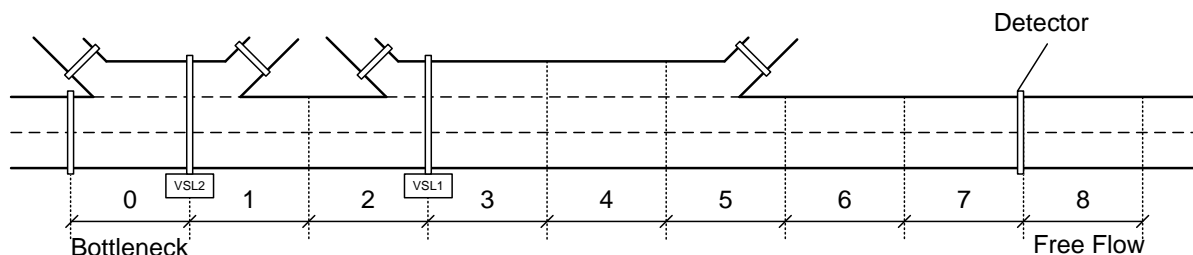


FIGURE 6(C) Illustration of freeway segmentation and VSL location

Based on the observed congestion during peak-hours, a VSL control system, consists of two VSL signs, four freeway detectors and four ramp detectors, was installed between MD 713 and Coca-Cola Drive. Note that effect of VSL is to slow down drivers' speeds prior to their approaching the congestion area (i.e. merging/diverging area). Based on our field survey, the VSL signs are located 800 feet upstream of two detected congestion bottlenecks, as shown in FIGURE 6(C).

The tested period is from 6:00-8:00 AM, which corresponds to the morning peak period. As shown in FIGURE 6(A), the high-speed traffic, when encountering the downstream congestion, drops its speed rapidly, causing a significant shockwave impact. Due to the short distance between the

diverging (295N off-ramp) and merging (295N on ramp) points, the congestion compounded with weaving activities has resulted in a large capacity reduction at the bottleneck subsection.

To create a more congested downstream bottleneck for better evaluation of proposed models, the tested traffic flow pattern is adjusted according to the filed data. As shown in FIGURE 7, around 55 percent of traffic flows come from the upstream segment and the rest are from the MD 713 and 295 N on-ramp. Also, about 15 percent of the approaching flows take the route via bottleneck segment to the 295 S off-ramp, and the remaining 85 percent flows enter the downstream freeway.

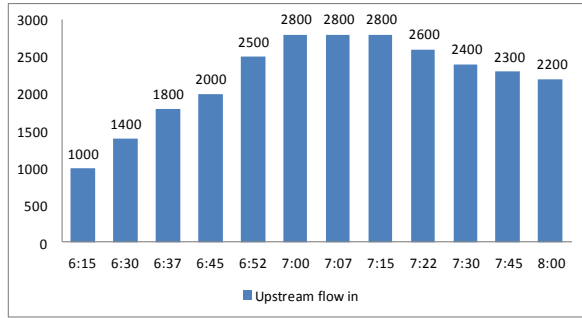


FIGURE 7(A) Time-varying approaching flows from upstream segment

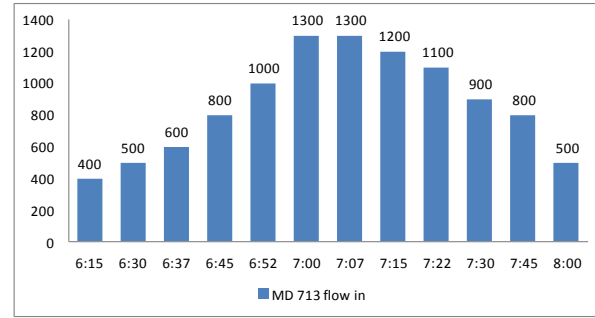


FIGURE 7(B) Time-varying approaching flows from MD 713

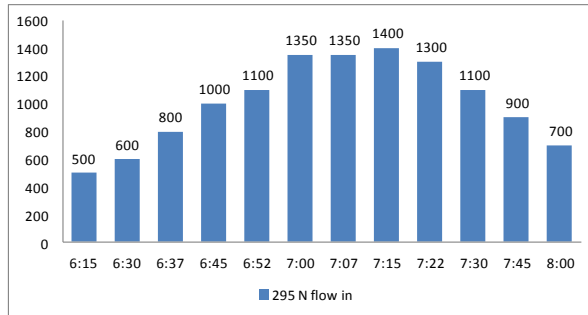


FIGURE 7(C) Time-varying approaching flows from 295 N on-ramp

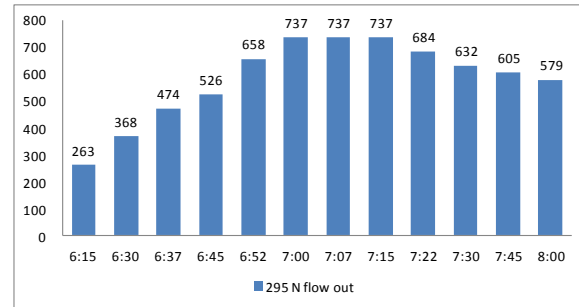


FIGURE 7(D) Time-varying leaving flows via 295 N off-ramp

Design of Simulation Tests and Parameter Selection

For performance evaluation, the micro-simulation software VISSIM, with its key parameters calibrated with data collected from our previous field study (7), is used as an unbiased platform. On the selected freeway segment (see FIGURE 6), our research group implemented two VSL signs, four sensors along with License-plate-recognition (LPR) system on Dec. 2009- Jan 2010. With the sensor data and real travel time information from the LPR, the calibration objective is to minimize the difference between simulated travel time and real travel time along the target freeway segment. For the car-following parameters, the max look ahead distance was calibrated to be 1000 ft, and the CC1 (headway time) was set as 0.80 s. Lane-changing parameters were also calibrated: the maximum deceleration is -20.11 ft/s^2 for own and -19.85 ft/s^2 for trailing vehicle; the accepted deceleration is -8.27 ft/s^2 and -6.63 ft/s^2 for own and trailing vehicle respectively; the waiting time before diffusion is 90 s.

To simulate the on-line VSL control with our proactive algorithms, this study has developed a VB.NET program to capture the online interaction between execution of the control algorithm and the time-varying traffic conditions. This mechanism has been programmed to enable our developed optimal VSL module to communicate with VISSIM during every simulation interval. Also note that the compliance rate of VSL is assumed to be 100% in this study.

To compare the proposed VSL models with No-control scenario, this study has designed the following four scenarios:

- Scenario-1: the basic proactive model with the objective of total travel time minimization;
- Scenario-2: the enhanced proactive model with the objective of total travel time minimization;
- Scenario-3: the basic proactive model with the objective of speed variance minimization; and
- Scenario-4: the enhanced proactive model with the objective of speed variance minimization.

The key model parameters for the experimental analysis are set as follows:

- The transition flow weigh factor α_i is 0.95;
- The Speed density adjustment factor β_i is 0.8;
- The congestion wave speed γ is 25 km/h;
- The Jam traffic density is 100 veh/lane/km;
- The Critical traffic density is 35 veh/lane/km;
- The free flow speed is 100 km/h;
- The allowed speed limit variance δ between two adjacent interval is 10 km/h;

Parameter v , τ , κ , calibrated by Wang (18), are 35 km/h, 20s and 13 veh/lane/km, respectively. Note that we full recognize the need to calibrate these parameters in field applications. However, this study presents our work at the exploratory stage, not for final model and for field application. Hence, our proposed model has directly taken the values of those parameters from the literature. Also, please note that those parameters adopted from the literature serve only as the initial values of the KF updating process, and thus its impact on the prediction results will be diminished over time when more and more data are detected from traffic sensors.

In the Kalman Filter model, the deviation of measurement errors for the flow rate and speed are selected from an extensive analysis of the experimental results and field data:

$$D(\varepsilon_i^q(k)) = 50 \text{ veh/h}, D(r_i^q(k)) = 50 \text{ veh/h}, D(s_i^q(k)) = 50 \text{ veh/h};$$

$$D(\varepsilon_i^u(k)) = 5 \text{ km/h};$$

The deviation of prediction errors for the flow rate and speed are assumed to be:

$$D(\xi_i^q(k)) = 250 \text{ veh/h}, D(\xi_i^u(k)) = 10 \text{ km/h}$$

Analysis of Experimental Results

Based on the objective of minimizing the total travel time, FIGURE 8(A) shows the distribution of mean speeds at the bottleneck segment-0 under Scenario-1, Scenario-2, and No-control scenario, revealing that the speeds under different scenarios are identical during the first hour (6:00-7:00AM)

due to the light traffic condition. However, during the peak hour (7:00-8:00AM), the traffic demands increase significantly and result in the downstream congestion. Comparing these three scenarios, it is clear that Scenario-2 can offer a higher speed (20 km/h) at the beginning of the congestion period (7:10-7:15AM), and maintain a more stable speed over the rest period (7:15-8:00AM) compared to the No-VSL control scenario. However, Scenario-1 (without update by the Kalman Filter method) fails to provide a proper control during the whole control period, which is due likely to its deficiency in offering an accurate traffic prediction and consequently unable to generate effective control speeds.

On contrast, FIGURE 8(B) represents mean speed evolution of the scenarios with the control objective of minimizing speed variance at the bottleneck. Obviously, Scenario-4 is able to maintain a stable bottleneck speed, starting from beginning of the traffic congestion period (7:00-8:00AM). Also, it can help reduced the congested duration, based on the speed evolution over the period (7:55-8:00AM). Scenario-3 can also offer acceptable control results. Compared with the No-Control scenario, the basic model was able to keep a higher speed at the beginning of congestion period (7:08-7:15AM), but lost its efficiency during the remaining period, as shown in FIGURE 8(B). The reason, as stated previously, is that the basic model is unable to capture the rapidly changing traffic condition and to revise the speed limit in time during the on-line applications.

Among all scenarios, the KF models with their proactive nature can always outperform the Basic models. Therefore, this study has further investigated the properties of these two KF models with different objective functions, and the results are shown in FIGURE 8(C).

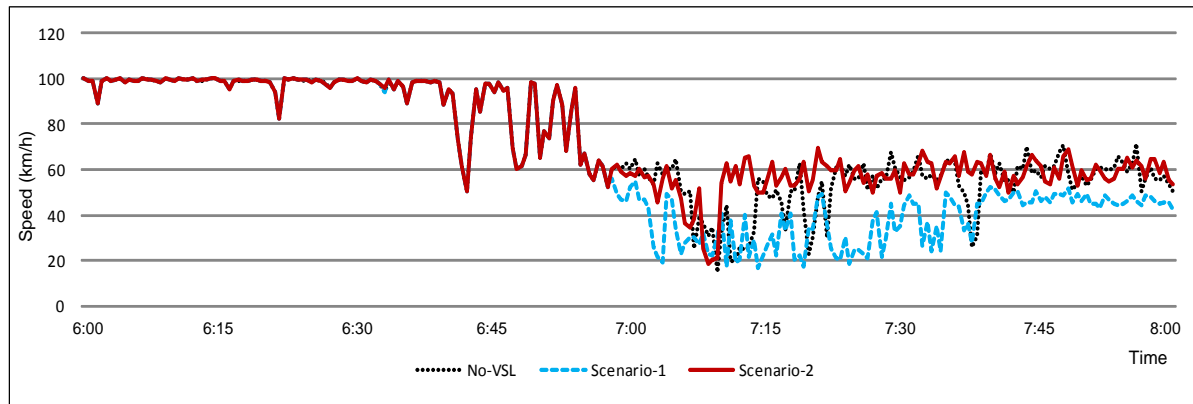


FIGURE 8(A) Mean speed at segment 0: Scenario 1,2 v.s. No-VSL scenario

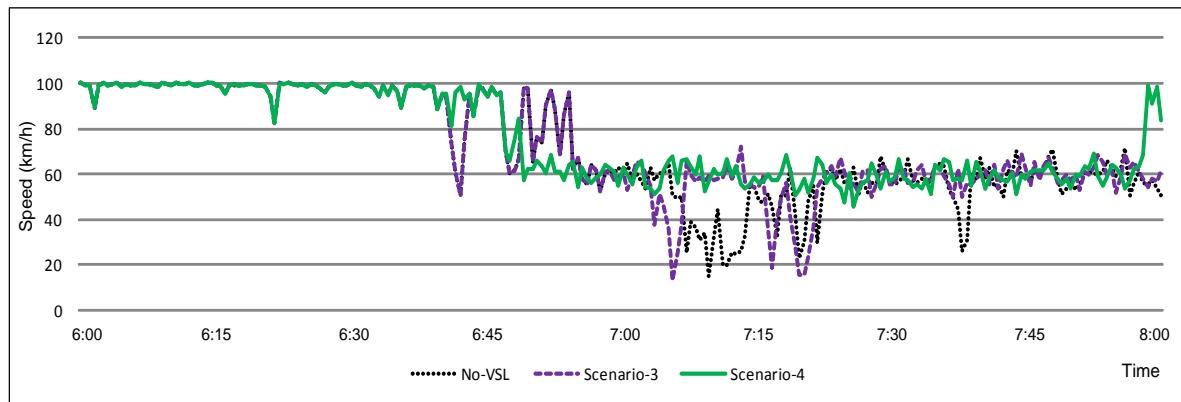
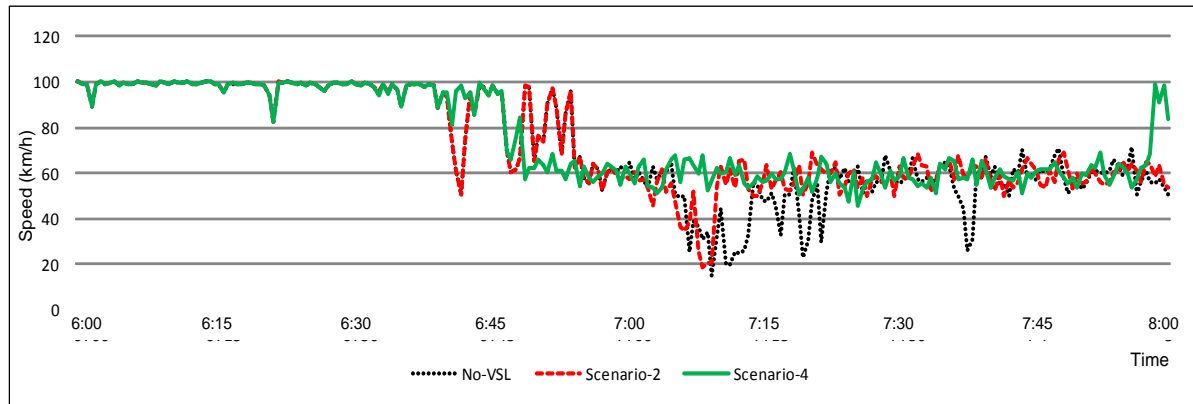
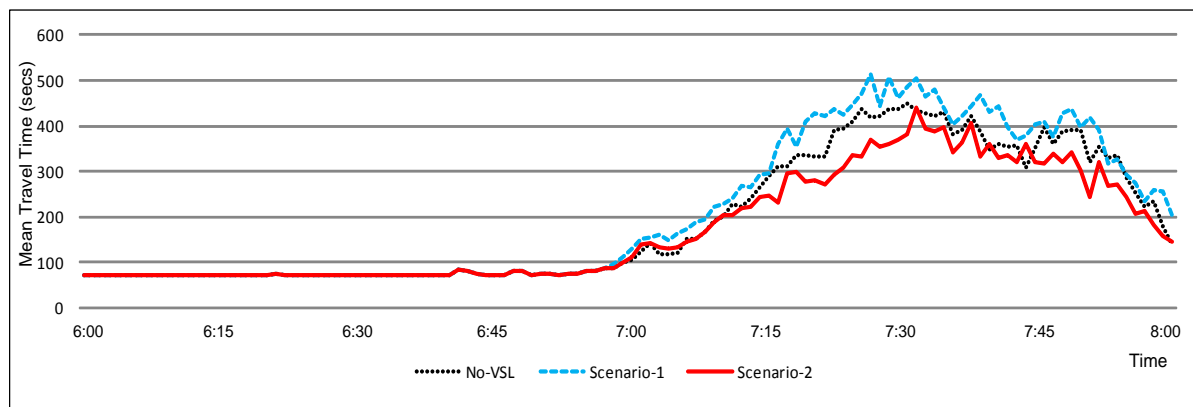


FIGURE 8(B) Mean speed at segment 0: Scenario 3,4 v.s. No-VSL scenario**FIGURE 8(C) Mean speed at segment 0: Scenario 2,4 v.s. No-VSL scenario**

As a major MOE to evaluate traffic efficiency, the time-dependant travel time can clearly reflect the effectiveness of each control strategy. FIGURE 9(A) presents the resulting travel time from these two models with the objective of minimizing travel time and the No-VSL scenario. Notably, the travel time starts to increase when the freeway is becoming congested (after 7:00AM). Compared with the No-control scenario, the average travel time is reduced by 70 seconds in Scenario-2, demonstrating the benefits under the VSL control. From FIGURE 9(B), it is clear that both speed-variance minimization models can reduce the travel time during the congested period (7:00-8:00AM). Also, the KF based model in Scenario-4 clearly outperforms the basic model in Scenario-3.

A further comparison between two KF models is shown in FIGURE 9(C). Note that during the period 6:45~7:00AM, Scenario-2 with the travel time minimization objective produces a lower travel time (20 secs on average) than Scenario-4 of minimizing the speed variance. However, as the congestion increases from 7:15AM, Scenario-4 begins to show better performance. To understand the reason of this interesting finding, we further analyzed the simulation process and found out that the variance-minimization model in Scenario-4 is more sensitive to the change in traffic conditions because it can immediately adjust the speed limit in advance even during the moderate congested period. The capability to sensitively adjust speed control in time can reduce the flow rate to the downstream segments, and consequently mitigate the potential shockwave impact.

**FIGURE 9(A) Time-dependent travel time: Scenario 1,2 v.s. No-VSL scenario**

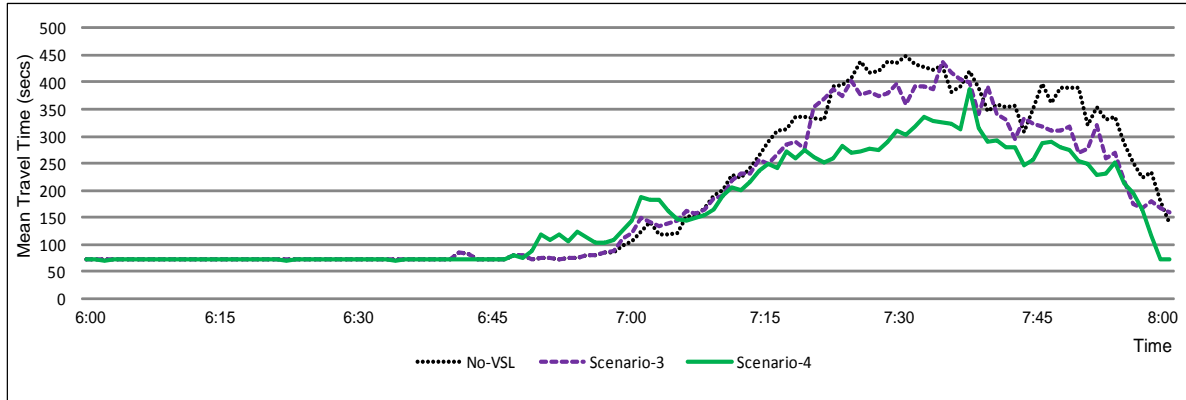


FIGURE 9(B) Time-dependent travel time: Scenario 3,4 v.s. No-VSL scenario

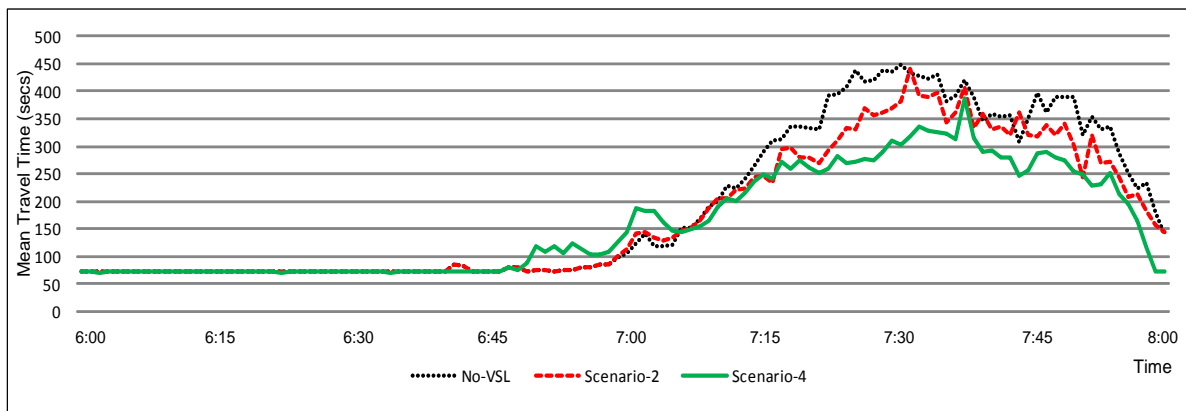


FIGURE 9(C) Time-dependent travel time: Scenario 2,4 v.s. No-VSL scenario

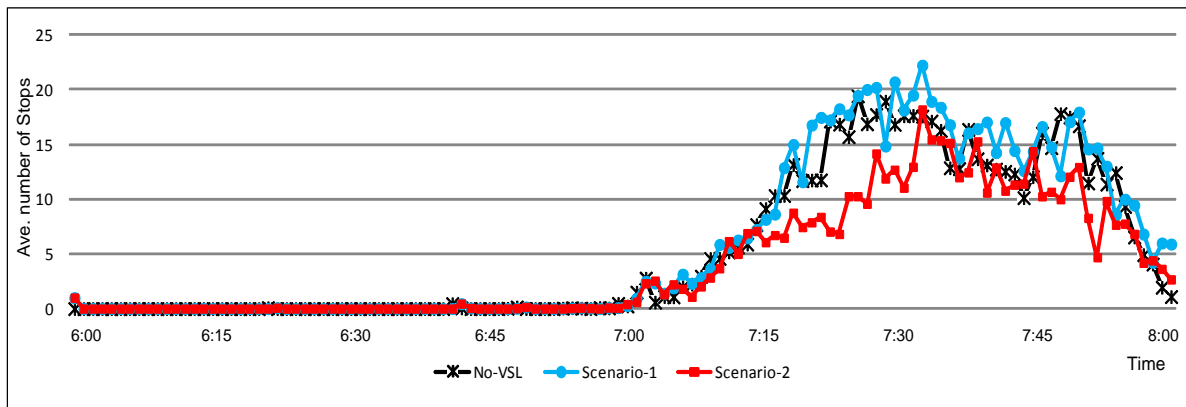


FIGURE 9(D) Time-dependent # of stops: Scenario 1,2 v.s. No-VSL scenario

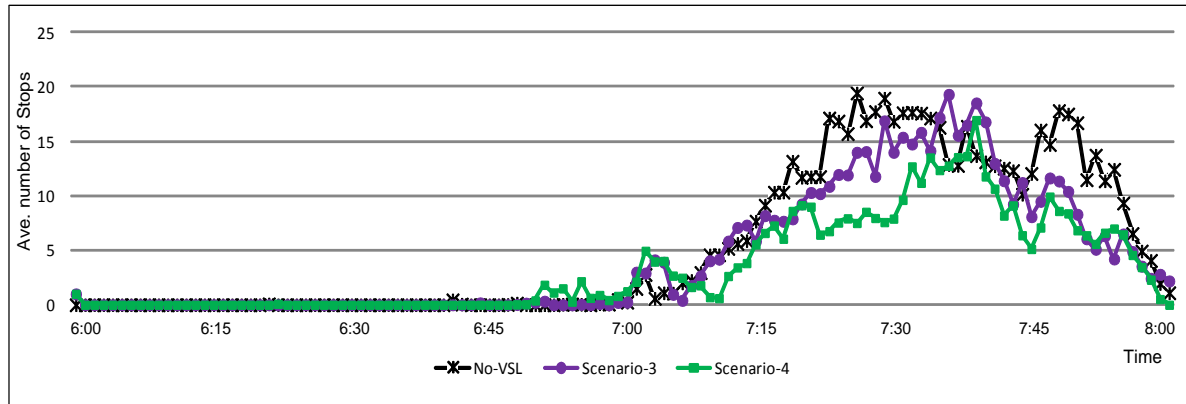


FIGURE 9(E) Time-dependent # of stops: Scenario 3,4 v.s. No-VSL scenario

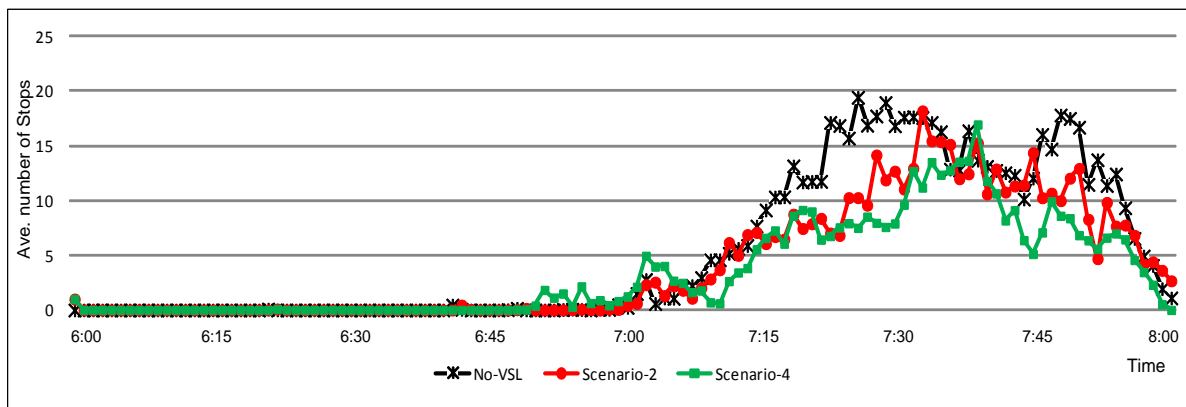


FIGURE 9(F) Time-dependent # of stops: Scenario 2,4 v.s. No-VSL scenario

As reported in the literature, an effective VSL system can reduce a driver's "stop-and-go" frequency. Therefore, the number of vehicle stops can also be viewed as an effective MOE for evaluating the efficiency of each proposed VSL system. FIGURE 9(D) ~ 9(F) also compare the time-dependent number of vehicle stops among different scenarios, and the results also indicate the promising property of the KF models, especially the one with the objective of minimizing speed variance (Scenario-4).

TABLE 1 summarizes the MOEs for all scenarios. To prevent the randomness of results, the data have been averaged over 10 simulation replications. Moreover, to distinguish the performance between the congested (7:00-8:00AM) and uncongested periods (6:00-7:00AM), TABLE 1 shows the overall results over the entire period and over the congested period. Notably, all three effective modes can yield significant reduction in both total travel time and vehicle stops. Among those three, Scenario-4 is the best one which yielded a reduction of 42.4 percent on the vehicle stops and 17.6 percent on the average travel time during the two-hour period. Scenarios-2 with its dynamic update function outperforms Scenario-3, and achieves a reduction in vehicle stops and travel time, respectively, by 19.9 percent and 9.6 percent.

TABLE 1 Performance Comparison between Different Scenarios

Scenario	6:00-8:00 Ave. # of Stops	Improvement	6:00-8:00 Ave. Travel Time	Improvement	7:00-8:00 Ave. Travel Time	Improvement
No-VSL	3.78	/	215	/	302	/
Scenario-1	4.23	11.9%	240	11.8%	344	13.7%
Scenario-2	3.03	-19.9%	194	-9.6%	270	-11.0%
Scenario-3	3.27	-13.53%	201	-6.2%	280	-7.6%
Scenario-4	2.18	-42.4%	177	-17.6%	235	-22.4%

In brief, one can tentatively reach the following preliminary conclusions from above experimental analysis:

- An inappropriate VSL system may deteriorate the traffic condition, as reflected by the increased travel and number of stops in Scenario 1;
- A proper VSL system can effectively reduce the number of stops and travel time over a recurrently congested freeway segment;
- The accuracy of the predicted traffic congestion can significantly affect the effectiveness of a VSL control system, as evidenced by the superior performance of two models with an embedded KF functions.
- The Kalman Filter is proved as a useful tool in the VSL system implementation as on traffic prediction model can fully capture the complex traffic dynamics.
- Speed variance minimization seems to be a better control objective, as the speed data is directly measurable from detectors and is the most sensitive variable to the VSL control.
- Speed variance minimization model is less sensitive to the prediction accuracy, as reflected in the performance evaluation results.

CONCLUSIONS AND FUTURE RESEARCH

In summary, this study has proposed two proactive VSL control models on recurrently congested freeway segments. The basic proactive model used embedded traffic flow relations to predict the evolution of congestion pattern and computed the optimal speed limit. To contend with the difficulty in capturing driver responses to VSL control, this study also proposed an advanced model with an embedded KF functions. Both models have been investigated with different traffic conditions and different control objectives. The extensive simulation analysis with VISSIM has revealed that both proactive VSL control models can significantly reduce the travel time and the number of vehicle stops over the recurrent bottleneck locations, and the one with minimizing speed variance as its control objective clearly outperforms other models, as reflected in the performance evaluation results.

Despite the acceptable performance of our proposed models at this exploratory stage, the authors full recognize that much remains to be done on this subject. One of our on-going tasks is to calibrate those important parameters based on field data. Also the sensitivity of the results to the traffic measurement errors is not answered in this study. Other on-going research tasks associated with VSL implementation include: exploring the potential of using multiple control objectives, identification of optimal detector locations for updating traffic conditions, and optimization of number of VMS speed displays for smoothing speed transition between the free-flow and the bottleneck traffic conditions.

1 REFERENCES

- 2 1. Steel, P., and R. McGregor. Application of Variable Speed Limits along the Trans Canada
3 Highway in Banff National Park. Presented at 2005 Annual Conference of the Transportation
4 Association of Canada, Calgary, Alberta, 2005.
- 5 2. Ulfarsson, G., and V. Shankar. The Effect of Variable Message and Speed Limit Signs on Mean
6 Speeds and Speed Deviations. *International Journal of Vehicle Information and Communication*
7 *Systems*, Vol. 1, No. 1–2, 2005, pp. 69–87.
- 8 3. Anund, A., and A. Ahlström. Evaluation of Local ITS Solutions in Urban Areas. No. 646.
9 Swedish National Road and Transport Research Institute, Linköping, Sweden, 2009.
- 10 4. Lyles, R. W., W. C. Taylor, and J. Grossklaus. Field Test of Variable Speed Limits in Work
11 Zones (in Michigan). Final Report RC-1467. Michigan Department of Transportation and
12 Michigan State University, Lansing, 2003.
- 13 5. Smulders, S., Control of freeway traffic flow by variable speed signs. *Transportation Research*
14 *Part B* 24 (2), 1990, pp. 111–132.
- 15 6. Bertini, R. L., S. Boice, and K. Bogenberger. Dynamics of Variable Speed Limit System
16 Surrounding Bottleneck on German Autobahn. In *Transportation Research Record: Journal of the*
17 *Transportation Research Board*, No. 1978, Transportation Research Board of the National
18 Academies, Washington, D.C., 2006, pp. 149–159.
- 19 7. Chang, G-L, S. Y. Park and J. Paracha. Intelligent Transportation System Field Demonstration
20 Integration of Variable Speed Limit Control and Travel Time Estimation for a Recurrently
21 Congested Highway. *TRR*, No. 2243, 2011, pp. 55-66.
- 22 8. Sisipiku, V. P., A. Sullivan, and G. Fadel. Implementing Active Traffic Management Strategies
23 in the U.S. University Transportation Center Report for Alabama, No. 08206, Birmingham, 2009.
- 24 9. Abdel-Aty, M., J. Dillmore, and L. Hsia. Applying Variable Speed Limits and the Potential for
25 Crash Migration. *TRR*, No. 1953, pp. 21–30.
- 26 10. Abdel-Aty, M., R. J. Cunningham, V. V. Gayah, and L. Hsia. Dynamic Variable Speed Limit
27 Strategies for Real-Time Crash Risk Reduction on Freeways. *TRR*, No. 2078, pp. 108–116.
- 28 11. Hegyi, A. Model predictive control for integrating traffic control measures. Ph.D. thesis, TRAIL
29 Thesis Series T2004/2, Delft University of Technology, Delft, The Netherlands, 2004
- 30 12. Heygi, A., B. De Schutter, and J. Hellendoorn. Optimal Coordination of Variable Speed Limits to
31 Suppress Shock Waves. *IEEE Transactions on ITS*, Vol. 6, No. 1, March 2005, pp. 102–112.
- 32 13. Papageorgiou, M., E. Kosmatopoulos, I. Papamichail. Effects of variable speed limits on
33 motorway traffic flow. *TRR*, No. 2047, 2008, pp. 37–48.
- 34 14. Carlson, R. C., I. Papamichail, M. Papageorgiou, and A. Messmer, Optimal motorway traffic
35 flow control involving variable speed limits and ramp metering, *Transportation Science*, vol. 44,
36 no. 2, pp. 238–253, 2010.
- 37 15. Hadiuzzaman, Md., Tony Z. Qiu. Cell Transmission Model Based Variable Speed Limit Control
38 for Freeway. Presented at 91th Annual Meeting of TRB, Washington, D.C., 2012.
- 39 16. Chang, G.-L., J. Wu, and H. Lieu. Real-Time Incident-Responsive System for Corridor Control:
40 Modeling Framework and Preliminary Results. *TRR*, No. 1452, TRB, 1994, pp. 42–51.
- 41 17. Wu, J., and G.-L. Chang. Heuristic Method for Optimal Diversion Control in Freeway Corridors.
42 In *Transportation Research Record: TRR*, No. 1667, TRB, 1999, pp. 8–15.
- 43 18. Wang, Y., M. Papageorgiou. Real-time freeway traffic state estimation based on extended
44 Kalman filter: a general approach. *Transportation Research Part B*, Vol. 39, No. 2, 2005, pp. 141-
45 167
- 46 19. Sims, A. G., and K. W. Dobinson. The Sydney Coordinated Adaptive Traffic (SCAT) System
47 Philosophy and Benefits. *IEEE Transactions on Vehicular Technology*, Vol. VT-29, No. 2, 1980,
48 pp. 130-137.